blood®
Regular Article

LYMPHOID NEOPLASIA

Targeted inhibition of CD47-SIRPα requires Fc-FcγR interactions to maximize activity in T-cell lymphomas

Salvia Jain,[1,2] Alexandria Van Scoyk,[3,4] Elizabeth A. Morgan,[2,5] Andrew Matthews,[1] Kristen Stevenson,[6] Gail Newton,[5] Foster Powers,[3] Anu Autio,[5] Abner Louissaint Jr,[2,7] Guillemette Pontini,[8] Jon C. Aster,[2,5] Francis W. Luscinskas,[2,5] and David M. Weinstock[2,3,9]

[1]Department of Medicine, Beth Israel Deaconess Medical Center, Boston, MA; [2]Harvard Medical School, Boston, MA; [3]Department of Medical Oncology, Dana-Farber Cancer Institute, Boston, MA; [4]Department of Oncological Sciences, University of Utah, Salt Lake City, UT; [5]Department of Pathology, Brigham and Women's Hospital, Boston, MA; [6]Department of Computational Biology and Biostatistics, Dana-Farber Cancer Institute, Boston, MA; [7]Department of Pathology, Massachusetts General Hospital, Boston, MA; [8]Novimmune SA, Geneva, Switzerland; and [9]Broad Institute of Harvard and MIT, Cambridge, MA

KEY POINTS

- CD47 surface protein expression is highly heterogenous, whereas MHC class I expression is homogeneous across T-cell lymphoma subtypes.
- Maximum antitumor efficacy from pharmacologic blockade of CD47 requires Fc-Fcγ receptor interactions.

Antibodies that bind CD47 on tumor cells and prevent interaction with SIRPα on phagocytes are active against multiple cancer types including T-cell lymphoma (TCL). Here we demonstrate that surface CD47 is heterogeneously expressed across primary TCLs, whereas major histocompatibility complex (MHC) class I, which can also suppress phagocytosis, is ubiquitous. Multiple monoclonal antibodies (mAbs) that block CD47-SIRPα interaction promoted phagocytosis of TCL cells, which was enhanced by cotreatment with antibodies targeting MHC class I. Expression levels of surface CD47 and genes that modulate CD47 pyroglutamation did not correlate with the extent of phagocytosis induced by CD47 blockade in TCL lines. In vivo treatment of multiple human TCL patient-derived xenografts or an immunocompetent murine TCL model with a short course of anti-CD47 mAb markedly reduced lymphoma burden and extended survival. Depletion of macrophages reduced efficacy in vivo, whereas depletion of neutrophils had no effect. F(ab′)2-only fragments of anti-CD47 antibodies failed to induce phagocytosis by human macrophages, indicating a requirement for Fc-Fcγ receptor interactions. In contrast, F(ab′)2-only fragments increased phagocytosis by murine macrophages independent of SLAMF7-Mac-1 interaction. Full-length anti-CD47 mAbs also induced phagocytosis by Fcγ receptor-deficient murine macrophages. An immunoglobulin G1 anti-CD47 mAb induced phagocytosis and natural killer cell-mediated cytotoxicity of TCL cells that was augmented by cotreatment with mogamulizumab, an anti-CCR4 mAb, or a mAb blocking MHC class I. These studies help explain the disparate activity of monotherapy with agents that block CD47 in murine models compared with patients. They also have direct translational implications for the deployment of anti-CD47 mAbs alone or in combination. (*Blood*. 2019;134(17):1430-1440)

Introduction

High expression of CD47 on tumor cells is believed to suppress phagocytosis by interaction with signal regulatory protein α (SIRPα) on macrophages and dendritic cells.[1-7] Several therapeutics, including ligand-blocking monoclonal antibodies (mAbs) to CD47 or SIRPα, engineered receptor decoys, and bispecific agents that disrupt the CD47-SIRPα axis, have demonstrated activity against preclinical models from a diverse spectrum of neoplasms.[1-10]

The agents currently in clinical trials can be divided based on their isotype backbone, CD47-binding component, and Fc domain. Hu5F9-G4, SRF231, and CC-90002 are all immunoglobulin G4 (IgG4) mAbs with functional Fc domains. Preliminary results from the first phase 1 study of Hu5F9-G4 in 58 patients with advanced cancers demonstrated tolerability but no clinical responses.[11] In contrast, the combination of Hu6F9-G4 with the anti-CD20 human IgG1 antibody rituximab demonstrated a complete remission rate of 36% in patients with rituximab-refractory diffuse large B-cell lymphoma or follicular lymphoma.[12]

TTI-621 is a soluble recombinant fusion protein consisting of the CD47-binding domain of human SIRPα linked to the Fc region of human IgG1.[13] Preliminary results in a phase 1 study of patients with cutaneous T-cell lymphoma (CTCL) demonstrated rapid reductions in both circulating lymphoma burden and severity of skin lesions with as little as a single intratumoral injection.[14]

ALX148 is another fusion protein comprising an engineered, high-affinity, CD47-binding domain of SIRPα linked to a modified human Fc domain that does not bind Fcγ receptors (FcγRs).[15] In a phase 1 study, 1 of the 24 evaluable patients

treated with single-agent ALX148 and 3 of the first 5 evaluable patients treated with ALX148 plus another antibody had stable disease as a best response.[16]

Together, these data suggest that a functional Fc region, and in particular an IgG1 isotype, may be required for maximal efficacy with CD47 blockade. These data also contrast with studies in murine models, which have shown impressive in vivo efficacy among agents that largely lack activity when given to patients as monotherapy.[1,2,11,17] Multiple additional molecules, including β-2-microglobulin/major histocompatibility complex (MHC) class I, SLAMF7, and factors that affect pyroglutamation of CD47 have recently been implicated as modulators of phagocytic responses that could affect the efficacy of CD47 blockade.[18-20]

We sought to address the role of human SIRPα and FcγRs in modulating the activity of CD47 blockade using primary samples and in vivo models of T-cell lymphoma (TCL). New therapies for these patients are desperately needed. Here we describe the molecular epidemiology and mechanistic contribution of factors involved in macrophage and natural killer (NK) cell responses induced by CD47 blockade across multiple TCL subsets.

Methods

Cell lines

Cell lines were acquired as previously described.[21] Additional details are provided in the supplemental Methods (available on the *Blood* Web site). All cell lines were routinely tested for mycoplasma detection with the MycoSEQ *Mycoplasma* Detection Assay from Applied Biosystems before use and authenticity was validated by short tandem repeat profiling.

CRISPR-Cas9 deletion of CD47 from Jurkat, MAC2A, and K-299 lymphoma cell lines

The human CD47 targeting lentivirus was generated using the vector lentiCRISPR v2 (Addgene plasmid #52961) expressing the guide sequence AATAGTAGCTGGAGCTGATCC. Transduced cell lines were cultured for 5 to 7 days in RPMI1640 supplemented with 20% fetal calf serum and L-glutamine before depletion of CD47-expressing cells using an anti-CD47 mAb (B6H12.2, ATCC) and magnetic beads coated with sheep anti-mouse IgG (Dynabeads, Life Technologies, Carlsbad, CA).

Therapeutic agents and antibodies

B6H12.2, MIAP410, and murine IgG1κ isotype controls were obtained from BioXCell. Nonblocking anti-human CD47 mAb, 2D3, was obtained from eBioscience and dialyzed to remove sodium azide. SRF231 and its human IgG4 isotype control were obtained from Surface Oncology. B6H12.2-hIgG1 antibody was obtained from Novimmune and its human IgG1 isotype control was obtained from Thermo Scientific. The therapeutic anti-CCR4 mAb, mogamulizumab (Moga) from Kyowa Kirin, anti-CD20 mAb, rituximab, anti-HER2 mAb, and trastuzumab were obtained through the clinical pharmacy at Dana-Farber Cancer Institute. The anti-human HLA-A, HLA-B, and HLA-C blocking antibody was generated from the murine hybridoma cell line, W6/32, which was obtained from ATCC (clone HB-95). Anti-human SLAMF7/CD319 (CRACC) antibody, clone 162.1 and its isotype, mouse IgG2aκ and IgG2bκ, and OKT3 were obtained from Biolegend.

RNA Sequencing

Analysis of RNA-sequencing (RNA-seq) data were implemented as recently described.[21] To permit analysis of the aggregated human peripheral blood mononuclear cell-derived T cells, TCL cell lines, and patient-derived xenograft (PDX) data, we first performed quantile normalization to adjust for library depth and platform-specific differences. Batch effects within PDX and cell lines were successfully removed using the ComBat approach from SVA 3.18.00.

In vivo models

In vivo studies were performed as previously described.[21] Additional details are included in the supplemental Methods.

Statistical methods

Details of the tissue microarray are included in the supplemental Methods. Progression-free survival (PFS) was calculated at the start of therapy postbiopsy to the time of progression or death censored at the date last known alive and compared using a log-rank test. Overall survival for PDX experiments was calculated from the time of treatment initiation to the time of death and compared using a log-rank test. Optimal splits of PFS were determined using the recursive partitioning package rpart in R version 3.5.0. A 2-sided Kruskal-Wallis (>2 group) or Wilcoxon rank-sum (2 group) nonparametric test was used to compare continuous measures for CD47%, intensity, and H score. Other continuous measures were compared between groups using a 2-sided Welch *t* test. Categorical comparisons were made between groups using a 2-sided Fisher exact test or for ordered categories a 2-sided Jonckheere-Terpstra test. *P* values were considered significant if $<.05$. Spearman and Pearson rank correlations were used to determine relationship between CD47, QPCTL, and PGPEP1 expression and sensitivity to phagocytosis mediated by CD47 blockade.

Results

CD47 is widely but heterogeneously expressed on the surface of human TCLs

Previous studies have reported that higher CD47 messenger RNA expression in biospecimens from patients with acute myeloid leukemia or B-cell non-Hodgkin lymphoma confers a poor prognosis.[1,2] Studies of messenger RNA expression can be highly problematic because they may not distinguish malignant cells and/or reflect surface protein expression. Thus, we examined CD47 protein expression on the surface of multiple TCL and B-cell lymphoma (BCL) lines and $CD3^+$ T cells from peripheral blood of healthy donors by flow cytometry. Differences in size between resting $CD3^+$ T cells (typically small) and transformed T cells (typically larger) could contribute to differences in fluorescence intensity by flow cytometry because larger cells presumably have greater overall surface area. Thus, normalizing to cell size would provide a more accurate marker of CD47 surface density. CD47 surface density on TCL from multiple subtypes was equivalent or higher in comparison with healthy $CD3^+$ T lymphocytes (Figure 1A). The surface density of CD47 on many TCL subtypes was comparable to Burkitt, diffuse large B-cell (DLBCL), and mantle cell lymphoma lines (Figure 1A). Similar results were confirmed by immunoblotting for total cellular CD47 (Figure 1B). Flow cytometry-based quantification of CD47 molecules per cell revealed

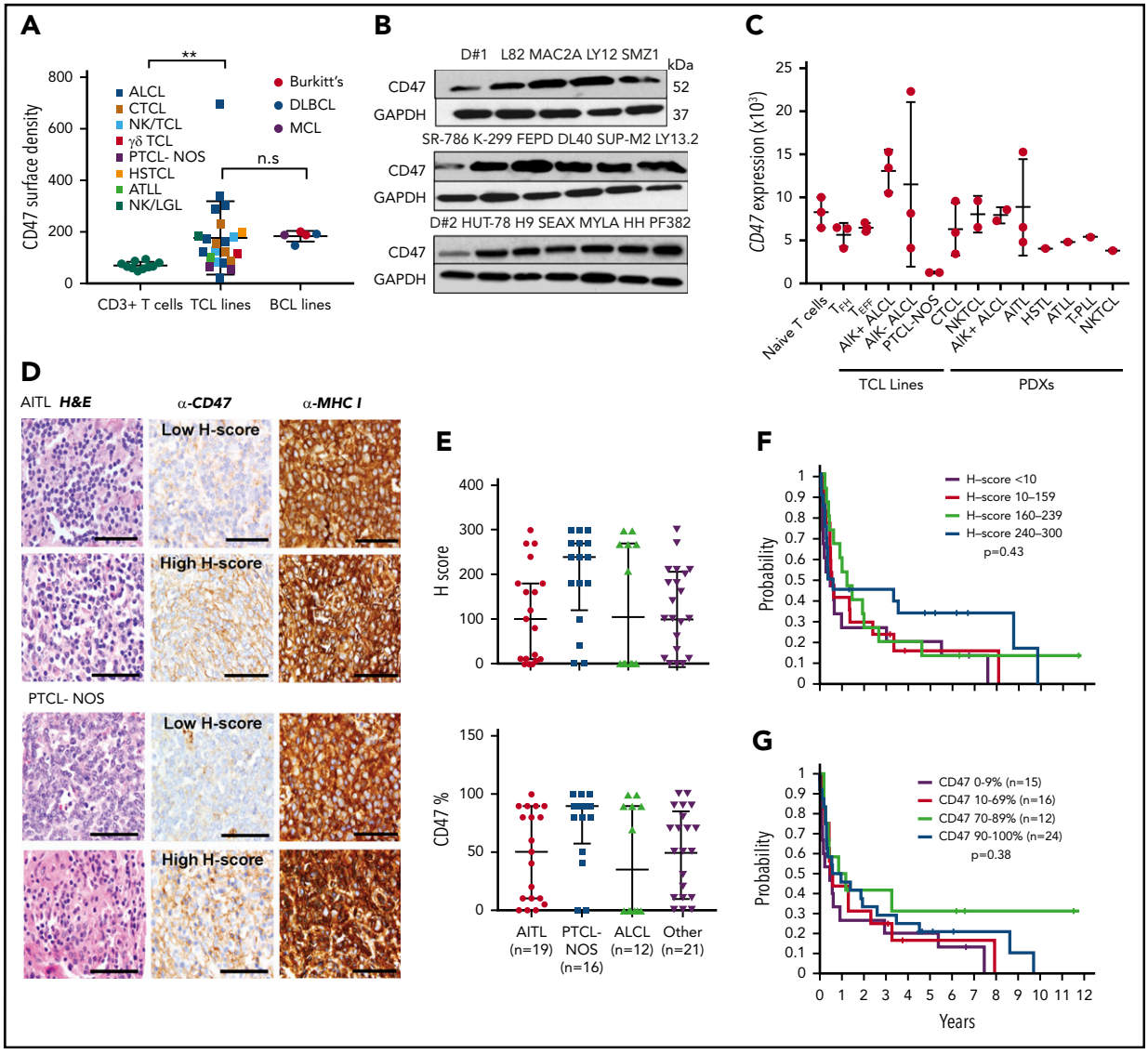

Figure 1. Human CD47 protein expression is heterogeneous, whereas MHC class I expression is homogeneous across TCL. (A) CD47 expression on normal peripheral blood-derived CD3⁺ T cells from healthy donors and TCL lines was determined by flow cytometry. CD47 surface density was plotted after mean fluorescence intensity was normalized for cell size. Each point represents a different healthy donor (n = 10) or TCL line (ALCL = 9 [DL-40, FEPD, KI-JK, L82, MAC2A, Karpas 299, SR-786, SU-DHL-1, SUP-M2], CTCL = 4 [HH, HuT-78, MJ, Myla], NKTCL = 3 [MTA, KHYG-1, SNK6], γδTCL [Karpas 384], HSTCL [DERL-2], PTCL-NOS = 2 [OCI-Ly12, SMZ-1], ATLL = 1 [HuT-102], and NKLGL = 1 [NKL]) or BCL line (Burkitt [Raji, Daudi], DLBCL [SU-DHL-2, SU-DHL-5, and Mantle cell [JVM-2]). **P = .0021 by 2-sided Welch t test. Normalized mean expression for each population was: CD3⁺ T cells 69.85 (range, 47.1-93.5) and TCL lines 176.9 (range, 20.9-694.8). (B) Resting CD3⁺ T cells from 2 additional donors (D#1, D#2) and TCL whole cell lysates were immunoblotted with the indicated antibodies. (C) Differential CD47 expression measured by RNA-seq was batch corrected and plotted. Three healthy donors were used for naïve, effector, and follicular helper T-cell groups. Cell lines: ALK+ ALCL = 3 (KI-JK, L82, SR-786), ALK- ALCL = 3 (MAC2A, OCI-Ly13.2, FEPD), PTCL-NOS = 2 (OCI-Ly12, SMZ-1), CTCL = 3 (HH, HuT-78, Myla), NK/TCL = 2 (KHYG-1, MTA). PDXs: ALK⁺ ALCL = 2 (WCTL-91953, WCTL-81162), AITL = 3 (DFTL-94393, DFTL-78024, DFTL-47880), HSTL = 1 (DFTL-81777), ATLL = 1 (DFTL-69579), T-PLL = 1 (DFTL-28776), and NK/TCL = 1 (DFTL-85005). (D) Representative images of patient lymph nodes stained for H&E, CD47 showing low and high H-scores and for MHC class I. Scale bar: 0.05 mm. (E) Histological analysis of CD47 expression in TCL patient-derived primary samples in the TMA (other: CTCL = 3, ATLL = 5, NK/TCL = 3, T-PLL = 1, subcutaneous panniculitis-like TCL = 2, γ/Δ TCL = 2, TCL unclassifiable = 3, and T-cell lymphoblastic lymphoma = 2). (F) PFS comparison between quartile groups by H-score (log-rank, P = .43). (G) PFS comparison between quartile groups by percent CD47⁺ lymphoma cells (log-rank, P = .38). H&E, hematoxylin and eosin.

comparable results across BCL and T-cell lymphoma lines in concert with the surface expression results (supplemental Figure 2A). We found heterogeneous expression of *CD47* transcript by RNA-seq across subsets of nonmalignant T cells, TCL lines, and TCL PDXs that also varied within each TCL subtype (Figure 1C).

To assess lymphoma cell CD47 protein expression in primary samples, we evaluated a 68-patient TMA that includes multiple TCL subtypes by immunohistochemical staining (Figure 1D). A full description of CD47 expression and extensive characterization of the TMA are included in supplemental Tables 1-5 and supplemental Figure 1A. The human anti-CD47 clone, 279, exhibited marked specificity for human CD47 protein based on staining of Jurkat wild-type (WT) and CD47-knockout cells and was selected for staining of the TMA (supplemental Figure 2B). We generated an H-score (defined as % of lymphoma cells that are CD47⁺ × intensity of CD47 staining from 0 to 3). We used the

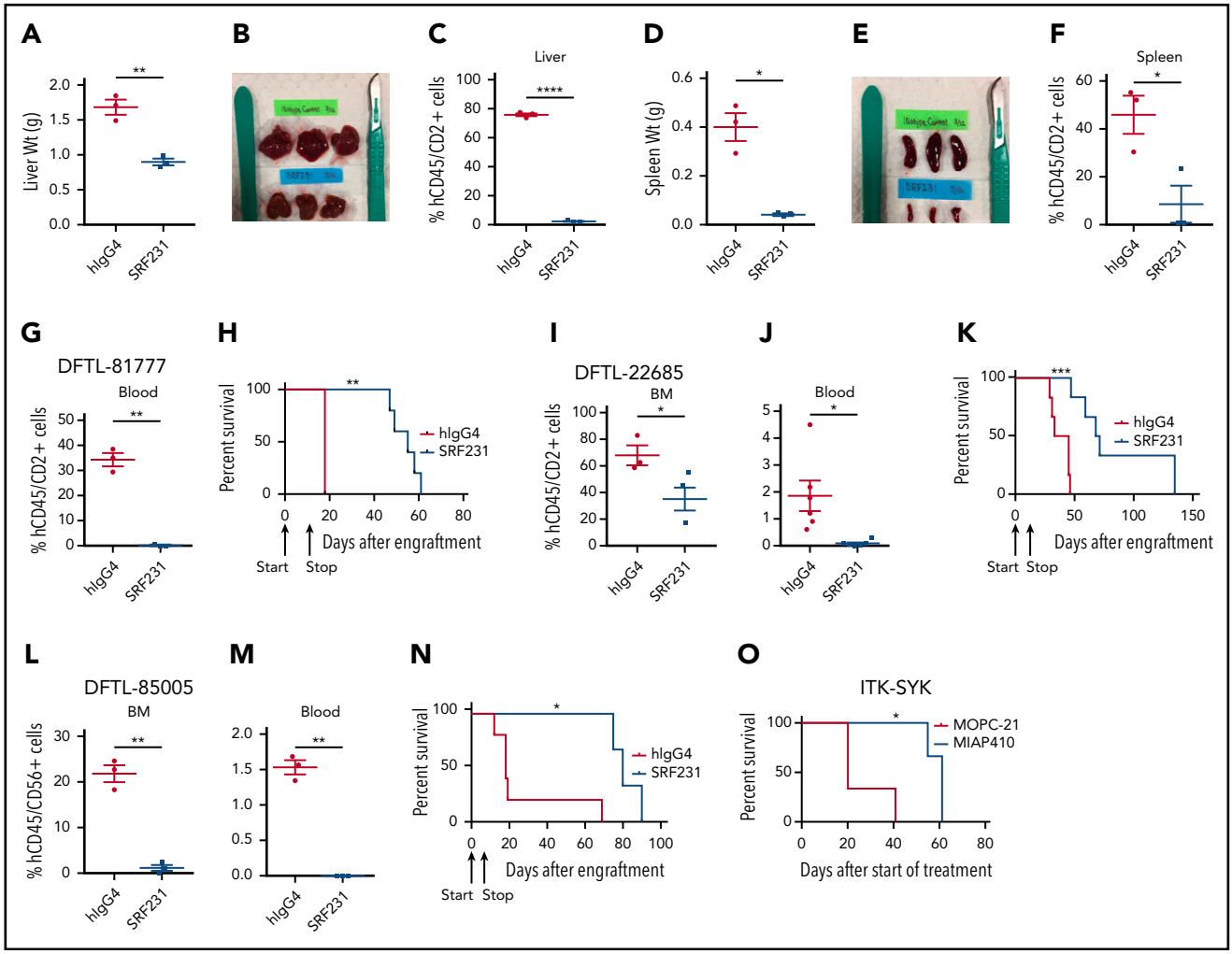

Figure 2. Therapy with anti-CD47 antibody SRF231 induces durable responses in TCL PDX and murine models in vivo. (A-F) Tumor burden and organ weights of mice engrafted with the HSTCL PDX DFTL-81777 and treated with hIgG4 isotype control or anti-CD47 antibody. (G-N) Tumor burden in blood and BM (n = 3 per antibody group). *$P < .05$; **$P < .01$; ***$P < .001$, ****$P < .0001$ by 2-sided Welch t test. Kaplan-Meier survival analyses (n = 3-6 per antibody group) by log-rank test. Arrows indicate start (day 0) and stop (day 10 for models 81777 and 22685) and start (day 0) and stop (day 4 for model 85005) of treatment. (O) Kaplan-Meier survival analysis of ITK-SYK xenograft model treated with murine anti-CD47 antibody, MIAP410, or with mIgG1κ isotype control, MOPC-21 (n = 3 per antibody group) log-rank test. BM, bone marrow.

maximum H-score among the multiple cores from each biopsy included in the TMA. H-score for CD47 expression was highly heterogeneous both within and across the common TCL subtypes (Figure 1E; $P = .17$ by Kruskal-Wallis test). The maximum percentage of lymphoma cells positive for CD47 membrane staining independent of intensity was also highly heterogeneous within and across the common TCL subtypes (Figure 1E; $P = .18$ by Kruskal-Wallis test). We further evaluated the spatial localization of CD47 expression by performing CD47 staining of the whole biopsy for multiple subtypes of TCL. We observed wide and ubiquitous expression of CD47 throughout the span of the biopsy (supplemental Figure 2C).

We divided patients into quartiles based on CD47 H-score and percentage of positive cells and compared their PFS from the time of their postbiopsy treatment. There were no significant differences in PFS across CD47 H-score quartiles (Figure 1F; $P = .43$) or across quartiles based on percentage of CD47$^+$ lymphoma cells (Figure 1G; $P = .38$). We applied a recursive partitioning approach but were unable to identify an optimal split based on CD47 H-score or percentage of CD47$^+$ lymphoma cells that resulted in a significant difference in PFS between groups (supplemental Figure 1B-E). There were also no significant associations detected between percentage of CD47$^+$ lymphoma cells (divided into 2 cohorts: above or below the median) and other prognostic variables such as international prognostic score or disease stage (supplemental Table 1).

Expression of the MHC class I common component β_2-microglobulin on the surface of cancer cells can suppress phagocytosis through interaction with the macrophage receptor, LILRB1.[18] Mutations of β_2-microglobulin that result in loss of MHC class I expression occur in ~30% of DLBCLs but are uncommon in TCLs.[22] We evaluated expression of MHC class I antigens on TCL cells in the TMA by immunohistochemical analysis. There was ubiquitous expression of MHC class I expression across the evaluable cores (Figure 1D). We confirmed this finding in a subset of samples by coimmunofluorescence staining for human MHC class I combined with CD4, CD8, or CD30 staining (supplemental Figure 2D).

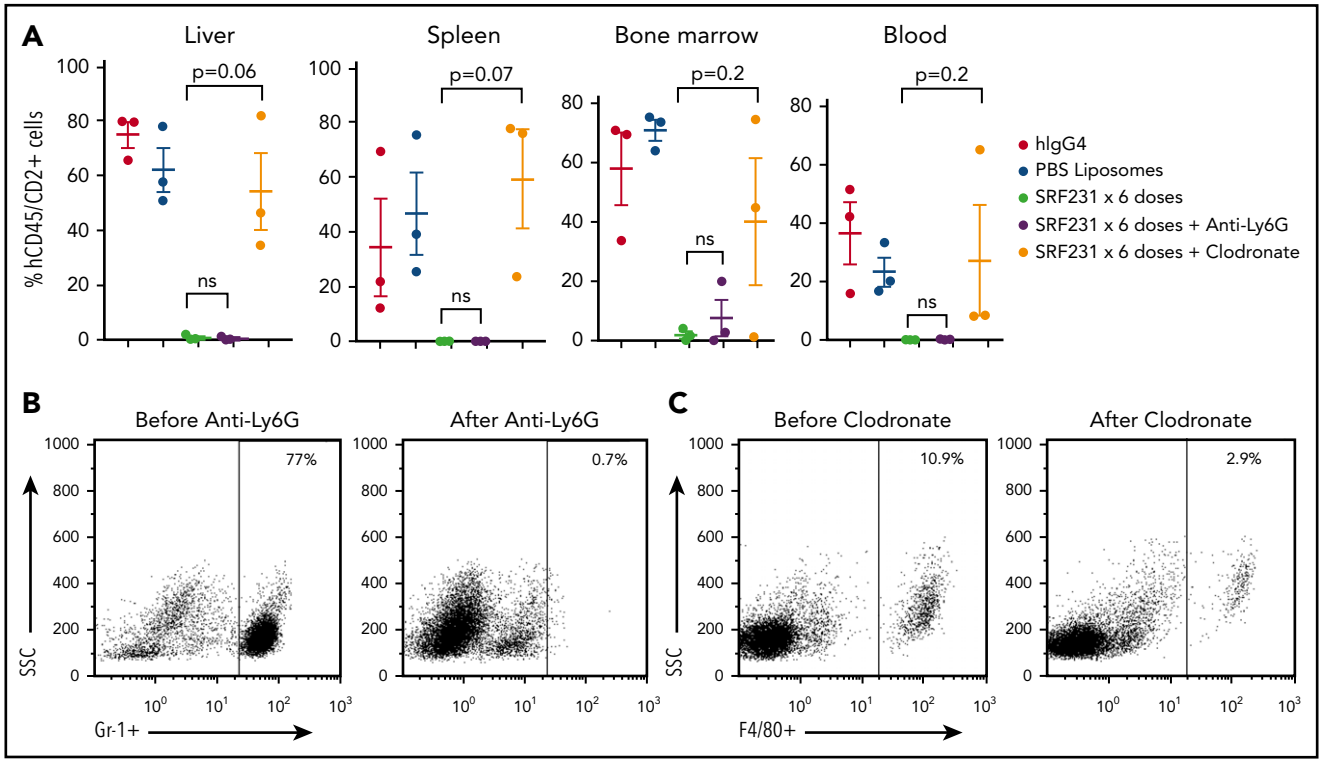

Figure 3. Anti-CD47 antibody efficacy is macrophage-mediated in TCL PDX. (A) Burden at involved sites for each mouse. *P* values by 2-sided Welch *t* test. (B) Flow plots of Gr-1$^+$ neutrophils in the peripheral blood of mice before and after treatment with anti-Ly6G Ab. (C) Flow plots of F4/80$^+$ macrophages in the peripheral blood of mice before and after treatment with clodronate. PBS, phosphate-buffered saline.

Anti-CD47 antibodies are highly active in disseminated PDX and immunocompetent models of TCL

The notable responses among patients with TCL to therapies that engage CD47 led us to test the fully human, clinical-grade anti-CD47 hIgG4 mAb SRF231 in vivo. Our laboratory has recently characterized several PDXs of TCL that engraft in the liver, spleen, bone marrow, lymph nodes, and/or blood.[21] We first used PDXs of hepatosplenic TCL (HSTCL; DFTL-81777) and transformed CTCL (DFTL-22685) with surface CD47 expression (supplemental Figure 3A-C). Upon engraftment with each PDX, mice were randomized to treatment with SRF231 or hIgG4 isotype control. Treatment with SRF231 with 6 doses (600 μg/dose) given on days 0, 2, 4, 6, 8, and 10 resulted in striking reductions in lymphoma involvement across compartments and markedly improved survival (Figure 2A-K; supplemental Figure 3D-F). In cocultures of fresh HSTCL cells taken from mice with murine bone marrow-derived macrophages (mBMDMs), exposure to SRF231 increased phagocytosis by twofold compared with isotype control (supplemental Figure 3G). Next, we assessed an abbreviated schedule using a PDX of NK/TCL (DFTL-85005). Treatment with only 3 doses of SRF231 (600 μg/dose) given on days 0, 2, and 4 also markedly reduced lymphoma burden and extended survival compared with isotype control (Figure 2L-N; supplemental Figure 3H-K).

To determine whether CD47 blockade is also effective in immunocompetent animals, we engrafted ITK-SYK-expressing lymphoma cells into syngeneic C57BL/6 mice.[23] Upon engraftment, treatment was initiated with the anti-mouse CD47 IgG1 mAb MIAP410 or isotype control (MOPC-21). MIAP410 also improved survival compared with isotype control (Figure 2O).

Anti-CD47 mAbs induce selective phagocytosis of TCL by macrophages

We sought to clarify the mechanisms through which CD47 blockade induces the profound in vivo effects noted previously. First, we depleted tumor-infiltrating macrophages and neutrophils from mice engrafted with human TCL in vivo. Depletion of murine Ly6G$^+$ neutrophils in NSG mice engrafted with the HSTCL PDX had no effect on the efficacy of SRF231 (Figure 3A-B). In contrast, coadministration of clodronate to deplete macrophages markedly reduced the activity of SRF231 across compartments (Figure 3A,C), consistent with macrophages being the primary effectors of anti-CD47 antibody therapy in the PDX models. To identify factors that may promote SRF231 activity in vivo, bone marrow lysates were collected from mice xenografted with the HSTCL and NKTCL PDXs on day 11 of treatment with SRF231 or hIgG4 and subjected to multiplex analysis of 65 human cytokines. Of all the cytokines quantified, the only human cytokine that significantly increased following treatment with SRF231 in both tumor models was interleukin-18 (IL-18; supplemental Figure 4A-B), a proinflammatory cytokine that can stimulate macrophage recruitment.[24] Next, we addressed whether CD47 blockade has a favorable therapeutic index for TCL cells compared with nonmalignant human T cells. CD3$^+$ T cells were isolated from the peripheral blood of healthy donors and confirmed to express CD47 (supplemental Figure 5A). As expected, the anti-CD52 hIgG1 mAb alemtuzumab increased phagocytosis of CD3$^+$ T cells by either mBMDMs or human monocyte-derived macrophages (hMDMs) in vitro

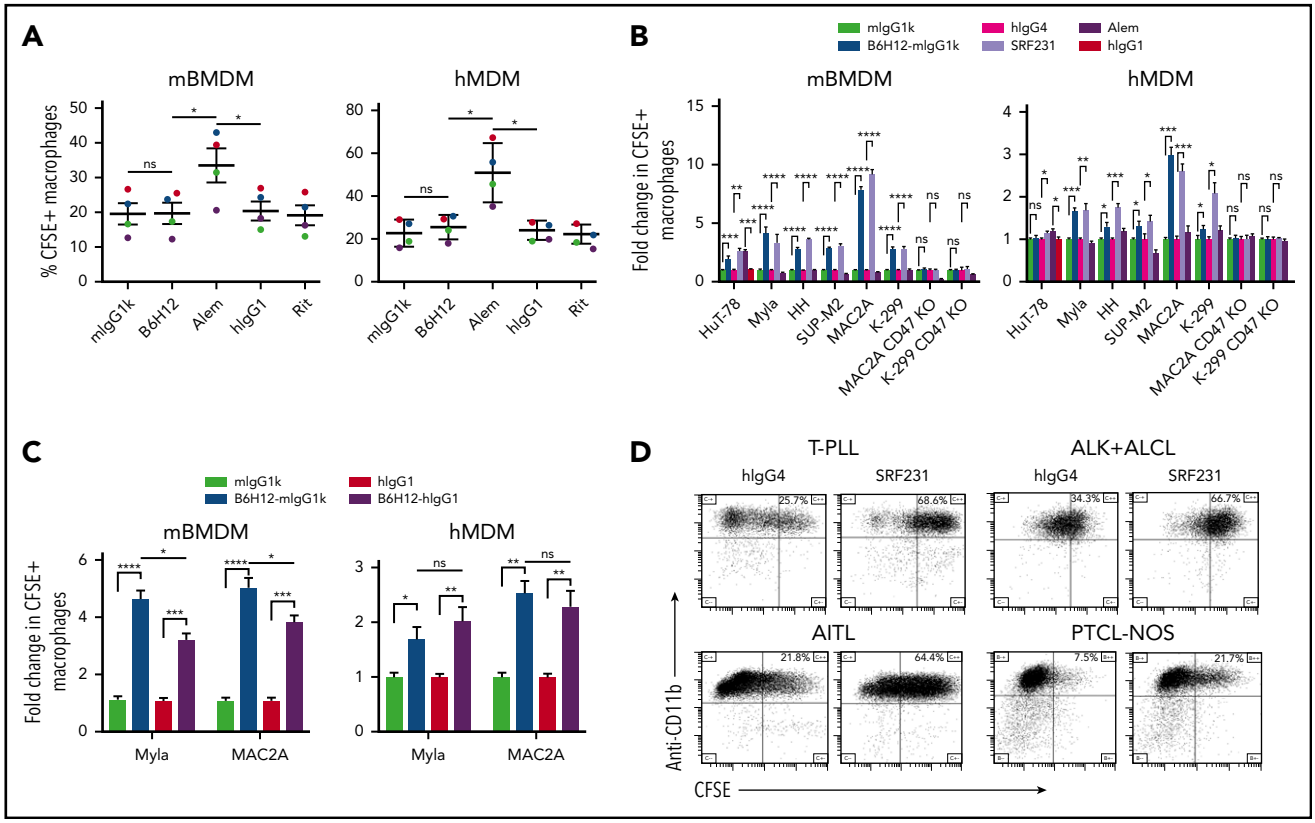

Figure 4. Anti-human CD47 monoclonal antibodies, B6H12 and SRF231 induce phagocytosis of TCL cells over nonmalignant T cells in vitro. (A) B6H12 induced phagocytosis of peripheral blood CD3$^+$ T cells from 4 healthy donors using mBMDM and hMDM in comparison with isotype control (mIgG1κ) are presented. The human anti-CD20 mAb rituximab (Rit) and anti-CD52 mAb alemtuzumab (Alem) both with hIgG1 isotype were used as negative and positive controls, respectively. (B, C) B6H12-mIgG1κ and SRF231 mediated phagocytosis of HuT-78, Myla, and HH (cutaneous T-cell lymphoma) and SUP-M2, MAC2A, Karpas 299 (K-299) (peripheral T-cell lymphoma) cells compared with isotype controls (mIgG1κ and hIgG4). Fold change in CFSE$^+$ of CD11b$^+$ mBMDMs and of CD14$^+$ hMDMs relative to the isotype control (mIgG1κ for B6H12-mIgG1κ, hIgG4 for SRF231, and hIgG1 for B6H12-hIgG1) for that cell line. Alemtuzumab was used as a positive control for induction of ADCP for CD52-expressing HuT-78 cell line and as a negative control for other lines. B6H12-mIgG1κ and B6H12-hIgG1 mediated phagocytosis of Myla and MAC2A relative to isotype controls is plotted for direct comparison between antibody isotypes. (D) Flow plots of mBMDM-engulfed CFSE$^+$ tumor cells with SRF231 and hIgG4 isotype control upon incubation of tumor cells ex vivo harvested from PDXs (ALK+ ALCL [WCTL-81162], T-PLL [DFTL-28776], AITL [DFTL-47880], and PTCL-NOS [DFTL-84867]).

(Figure 4A). B6H12 did not increase phagocytosis of CD3$^+$ T cells (Figure 4A), but both B6H12 and SRF231 enhanced phagocytosis of several TCL lines (Figure 4B; supplemental Figure 5B). There was no correlation between level of surface CD47 expression and the induction of phagocytosis upon exposure to anti-CD47 antibodies across TCL lines (supplemental Tables 6 and 7; supplemental Figure 5C). A recent study demonstrated that pyroglutamation of CD47 is critical for interaction with SIRPα.[20] However, the expression level of neither the enzyme that catalyzes CD47 pyroglutamation (QPCTL) nor the aminopeptidase that reverses it (PGPEP1) correlated with the induction of phagocytosis upon exposure to anti-CD47 antibodies (supplemental Figure 5C).

We generated CD47-null versions of MAC2A and K-299 by CAS9-mediated transgenesis (supplemental Figure 5D). Both lines had enhanced susceptibility to phagocytosis by mBMDMs and hMDMs compared with their WT counterparts (supplemental Figure 5B). As expected, B6H12 or SRF231 did not increase phagocytosis of the CD47-null cell lines relative to isotype controls (Figure 4B). We noted that B6H12 is a murine IgG1, whereas SRF231 is a human IgG4. To directly compare across antibody species, we also tested a B6H12 engineered to have a human IgG1 Fc. B6H12-mIgG1 induced slightly greater phagocytosis of human TCL lines compared with B6H12-hIgG1 by mBMDMs (Figure 4C). These differences are likely due to differences in Fc-FcγR affinities across species.

To directly confirm that SRF231 induces phagocytosis of TCL PDX cells by BMDMs, we isolated live TCL cells from mice. We confirmed that these cells express surface hCD47 (supplemental Figure 5D), labeled them with carboxyfluorescein diacetate succinimidyl ester (CFSE), and cocultured them ex vivo with mBMDMs. SRF231 increased phagocytosis of all 4 PDXs relative to hIgG4 isotype control (Figure 4D). Thus, the induction of phagocytosis with murine mAbs targeting CD47 appears to be largely isotype and species independent.

Anti-CD47 mAbs induce antibody-dependent cellular cytotoxicity of TCL

Previous studies have suggested that CD47 engagement may induce other mechanisms of cell killing beside antibody-dependent cellular phagocytosis (ADCP).[2] Incubation of TCL cells with B6H12 or B6H12-hIgG1 had minimal effects on apoptosis (Figure 5A). Similarly, there was no induction of complement-dependent cytotoxicity (CDC) of TCL cells with either murine or human complement upon exposure to B6H12 (Figure 5B) or B6H12-hIgG1 (Figure 5C).

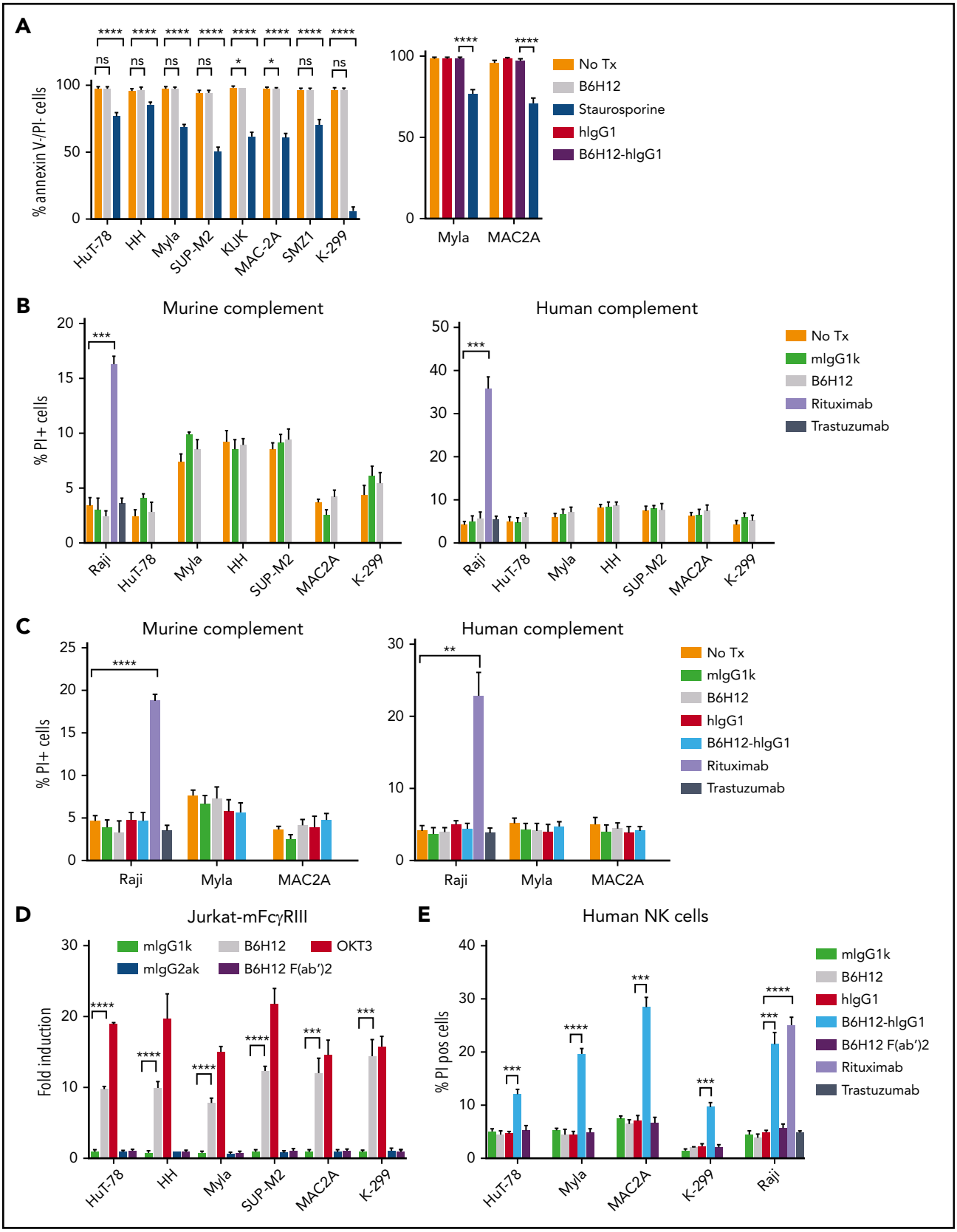

Figure 5. Anti-CD47 monoclonal antibodies exert minimal apoptosis, no CDC, but affect ADCC. (A) TCL cells were incubated with the indicated antibodies at 10 μg/mL or 10 μM staurosporine (positive control) for 2 h and the percentage of live cells was quantified by flow cytometry. (B, C) CDC assay with 30% murine and human complement was performed in triplicate and % PI^+ cells are reported. Rituximab and Raji cells were used as positive controls, whereas trastuzumab was used as negative control. (D) ADCC reporter assay measuring luminescence with murine FcγRIIIA-expressing Jurkat cells was performed in triplicate at an effector:target ratio of 25:1 with indicated antibodies. Human anti-CD3 mAb (OKT3) was used as positive control along with its isotype control, mIgG2aκ. Fold induction is relative to isotype control (mIgG1κ for B6H12 and mIgG2aκ

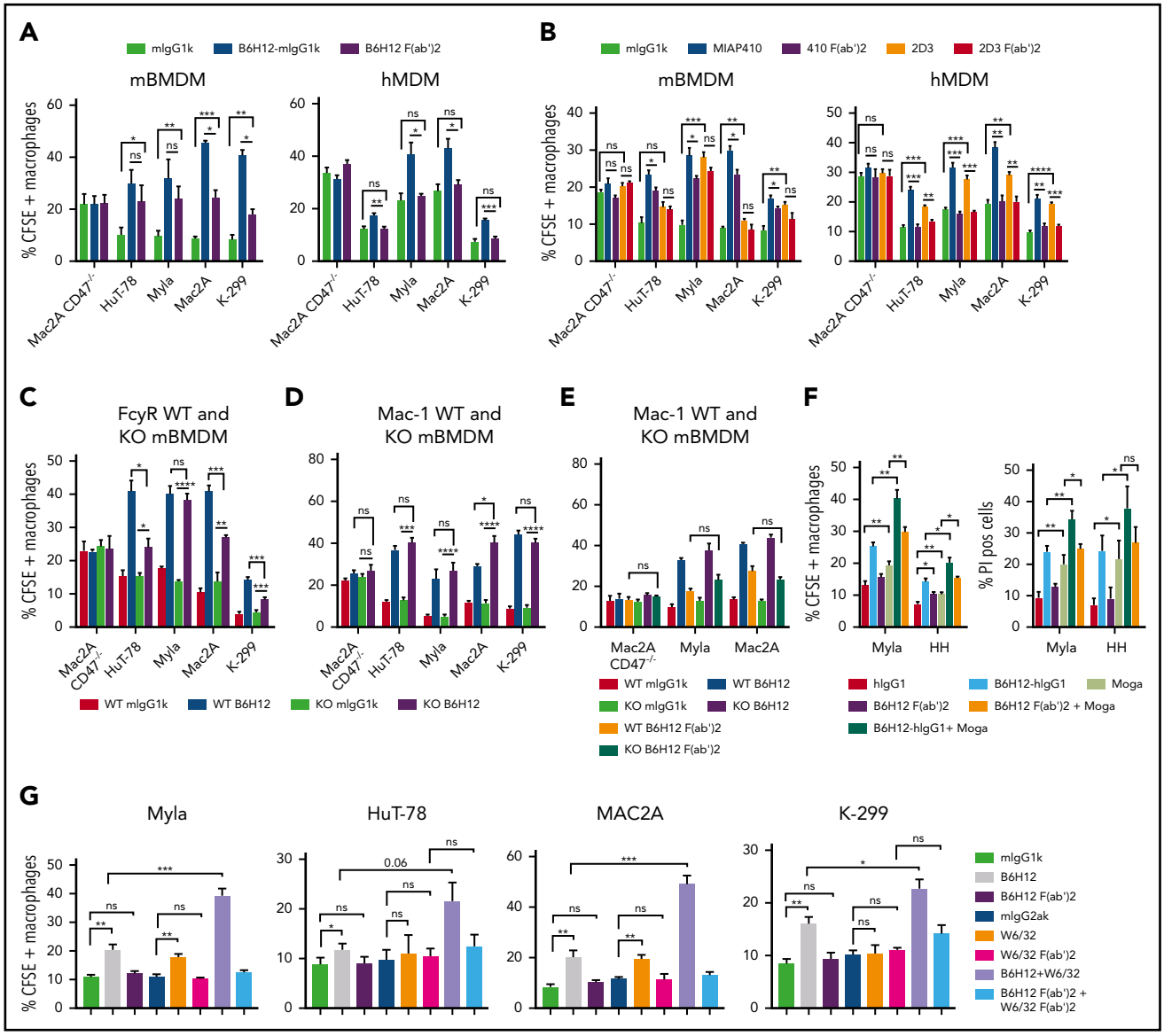

Figure 6. Anti-CD47 antibody increases phagocytosis through Fcγ*R*-independent and Fcγ*R*-dependent mechanisms and is not Mac-1 dependent. (A) CFSE$^+$ TCL cells were incubated in vitro with B6H12 and F(ab')2 fragment of B6H12 or isotype control in the presence of mBMDMs and hMDMs. (B) Same as panel A, using full-length and F(ab')2 fragments of 2D3 and MIAP410. (C) CFSE$^+$ TCL cells were incubated with WT or *Fcer1g*$^{-/-}$ (KO) mBMDMs in the presence of the indicated antibodies. Shown are mean values of technical triplicates with error bars representing SEM. *$P < .05$, **$P < .01$, ***$P < .001$, ****$P < .0001$ by 2-sided Welch *t* test. (D-E) CFSE$^+$ TCL cells were incubated with WT or *Mac1*$^{-/-}$ (KO) mBMDMs in the presence of the indicated antibodies or F(ab')2 fragment of B6H12. A representative experiment performed in triplicate with error bars representing SEM is shown. (F) On the left, phagocytosis of CFSE-labeled CTCL cells, Myla and HH by hMDMs in the presence of various antibodies including Moga at concentrations of 5 μg/mL is plotted. On the right, percent PI positive of the CFSE-labeled Myla and HH cells is plotted after culture with human NK cells in the presence of various antibodies at concentrations of 10 μg/mL. Shown are mean values of technical triplicates with error bars representing SEM. *$P < .05$, **$P < .01$, ***$P < .001$, ****$P < .0001$ by 2-sided Welch *t* test. (G) Phagocytosis of Myla, HuT-78, MAC2A, and K-299 cells mediated by full-length B6H12-mIgG1κ, anti-HLA A,B,C mAb, W6/32 and their F(ab')2 portions alone and in combination relative to isotype controls at 10 μg/mL (mIgG1κ for B6H12-mIgG1κ and mIgG2aκ for W6/32). Percentage of CFSE$^+$ macrophages (of CD14$^+$ hMDMs) is plotted. Shown are mean values of technical triplicates ± SEM. *$P < .05$; **$P < .01$; ***$P < .001$, ****$P < .0001$ by 2-sided Welch *t* test. KO, knockout; ns, not significant.

To assess antibody-dependent cellular cytotoxicity (ADCC), we took 2 different approaches. First, we used an established assay involving Jurkat cells that express murine FcγRIII, the primary FcR on murine NK cells involved in ADCC. ADCC of all TCL lines by these Jurkat cells was increased by adding B6H12 or the positive control antibody OKT3 (Figure 5D). To test whether

Figure 5 (continued) for OKT3). Shown are mean values of technical triplicates with error bars representing SEM. *$P < .05$, **$P < .01$, ***$P < .001$, ****$P < .0001$ by 2-sided Welch *t*-test. (E) CFSE-labeled TCL cells were incubated with human-derived NK cells in the presence of indicated antibodies for 4 hours. Percentage of propidium iodide positive (% PI pos) (of CFSE$^+$) cells was determined by flow cytometry and plotted. Rituximab and Raji cells were used as positive controls whereas trastuzumab was used as negative control. Shown are mean values of technical triplicates with error bars representing SEM. *$P < .05$, **$P < .01$, ***$P < .001$, ****$P < .0001$ by 2-sided Welch *t* test. SEM, standard error of the mean.

B6H12-mediated ADCC was Fc-dependent, we generated a F(ab')2 fragment of B6H12. The F(ab')2 fragment did not increase ADCC compared with isotype antibody (Figure 5D), indicating that the increased ADCC induced by B6H12 was mediated through Fc-FcγR interactions.

In the second assay, we directly tested ADCC of TCL cells by human NK cells. Neither the F(ab')2 fragment nor the murine B6H12 induced ADCC by human NK cells (Figure 5E). However, the B6H12-hIgG1 potently induced ADCC of TCL cells and of the BCL line Raji (Figure 5E). These findings underscore the importance of Fc-FcγR interactions in ADCC induced by mAbs that bind CD47.

ADCP induced by CD47 blockade differs across species based on the contribution of Fc interactions

Next, we asked whether Fc interactions are required for the induction of ADCP by mAbs targeting CD47. Using mBMDMs, the F(ab')2 fragment of B6H12 increased phagocytosis of TCL lines compared with isotype control, but not to levels equivalent to full-length B6H12 (Figure 6A). Strikingly, the F(ab')2 fragment of B6H12 induced minimal or no phagocytosis of TCL lines by hMDMs above the level of isotype control (Figure 6A). As expected, neither full-length B6H12 or the F(ab')2 fragment promoted phagocytosis of CD47-knockout MAC2A cells by mBMDMs or hMDMs.

To confirm the importance of Fc-FcγR interactions, we assessed full-length and F(ab')2 fragments of other anti-CD47 mAbs.[1] The addition of either full-length MIAP410 or full-length 2D3 promoted phagocytosis of TCL cells by mBMDMs or hMDMs (Figure 6B). As with B6H12, the F(ab')2 fragments of either antibody only promoted phagocytosis of TCL cells by mBMDMs. Increased concentrations of B6H12-F(ab')2 up to 50 μg/mL did not enhance the phagocytosis of the TCL cells by human macrophages (supplemental Figure 6A). Concentrations of the full-length or F(ab')2 portion of B6H12 as low as 1 μg/mL essentially saturated CD47 (supplemental Figure 6B), suggesting that further increases in the concentration of the F(ab')2 fragment would not yield greater phagocytic activity. Thus, the requirement for a functional Fc portion to induce phagocytosis by human macrophages appears to extend across anti-CD47 mAbs.

We then used macrophages from *Fcer1g*$^{-/-}$ mice, which lack expression of FcγRI, FcγRIII and FcεRs.[25] Consistent with the data using B6H12 F(ab')2, full-length B6H12 increased phagocytosis of TCL lines by *Fcer1g*$^{-/-}$ macrophages but less than compared with WT macrophages (Figure 6C). Thus, phagocytosis of TCL cell lines by murine macrophages induced by anti-CD47 antibody involves both Fcγ*R*-dependent and Fcγ*R*-independent mechanisms.

SLAMF7-MAC1 interaction is not required for TCL phagocytosis induced by CD47 blockade

A recent study reported that phagocytosis of human B-lymphoid, murine B-lymphoid, and murine myeloid tumor cells induced by CD47 blockade absolutely requires homotypic expression of SLAMF7 both in vitro and in vivo.[18] SLAMF7 in the tumor cells promoted phagocytosis by engaging immunoreceptor tyrosine-based activation motif-containing proteins on macrophages such as DAP12 and FcγRs, which mediate immune cell activation via Syk, Btk, and SRC kinases. SLAMF7 interacted with the integrin Mac-1 to trigger phosphorylation of immunoreceptor tyrosine-based activation motif motifs.[18] We therefore investigated whether CD47-mediated phagocytosis of TCL cells was dependent on SLAMF7-Mac-1 interaction. Although CD3^{+} T cells expressed surface SLAMF7, 5 of 5 TCL cell lines tested lacked any discernible SLAMF7 surface expression compared with isotype control (supplemental Figure 7).

We next tested phagocytosis using mBMDMs from WT and *Itgam*$^{-/-}$ (Mac1-deficient) mice.[26] There were no significant differences in the extent of phagocytosis between WT and *Itgam*$^{-/-}$ macrophages induced by full-length B6H12 (Figure 6D) or by the F(ab')2 fragment of B6H12 (Figure 6E). Thus, SLAMF7 on tumor cells and Mac-1 on mBMDMs are expendable for CD47 blockade-dependent phagocytosis of TCL cells. Similar findings were recently reported by for BCL.[27]

To further test if opsonization of TCL cells with therapeutic antibodies enhances their phagocytosis and cytotoxicity by effector cells in the presence of anti-CD47 antibodies, we performed experiments with B6H12-hIgG1 mAb in combination with Moga, the anti-CCR4 humanized IgG1 antibody recently approved in the United States for use in patients with relapsed and refractory CTCL and approved in Japan for adult TCL/lymphoma.[28] The combination of full length anti-CD47 and anti-CCR4 mAbs enhanced both phagocytosis by human macrophages and ADCC of the CTCL cells by human NK cells relative to either antibody alone (Figure 6F).

We noted that the full-length B6H12 combined with Moga was more effective at induced both phagocytosis and ADCC compared with the F(ab')2 fragment of B6H12-hIgG1 combined with Moga (Figure 6F). This suggests that opsonization with 2 functional mAbs may be more efficacious than a single antibody. Thus, we assessed the combinatorial effects of mAb blockade of MHC class I on ADCP. Single-agent treatment with the W6/32, a murine IgG2 antibody that blocks human HLA-A, HLA-B, and HLA-C induced hMDM-mediated phagocytosis of 2 of 4 TCL lines (Figure 6G). This induction was not observed with a W6/32 F(ab')2 fragment (Figure 6G). Importantly, the combination of a W6/32 F(ab')2 and a B6H12 F(ab')2 also did not significantly induce phagocytosis by hMDMs, indicating that coblockade of MHC class I and CD47 is not likely to be effective without functional Fc-FcγR interactions. In contrast, full-length W6/32 combined with full-length B6H12 induced synergistic (ie, greater than additive) increases in phagocytosis across all 4 lines (Figure 6G).

Discussion

Our results indicate that recruitment of effector cells such as macrophages or NK cells by engagement of FcγRs is critical for maximizing the efficacy of CD47-blocking therapies. Our observations also suggest that the nature of innate immune response upon CD47 blockade depends on the isotype backbone of the blocking antibody. A hIgG1 anti-CD47mAb can induce both ADCP and ADCC of tumor cells, which might partly explain the clinical efficacy observed with single-agent TTI-621 in patients with CTCL.

Previous studies have reported direct effects of disrupting the CD47-SIRPα axis that were purportedly autonomous from Fc-FcγR interactions.[2] However, this was based on studies with human CD47 and murine SIRPα. Our data revealed that, in the context of human macrophages, blockade of CD47-SIRPα

interaction alone is suboptimal for inducing phagocytosis and, in some cell lines, no more effective than a negative control. Our studies comparing full-length with F(ab')2 portions of anti-CD47 antibodies (with or without MHC class I or anti-CCR4 antibodies) confirm that the Fc portion is critical for maximally inducing effector responses.

We also observed a striking difference in the phagocytic vulnerability of CD47-null cells compared with pharmacologic disruption of the CD47-SIRPα axis using F(ab')2 portions of multiple antibodies. Both MAC2A and K-299 CD47-null cells displayed a marked sensitivity to macrophage engulfment compared with their WT counterparts. However, when the WT cells were treated with ligand-blocking concentrations of anti-CD47 F(ab')2 portions, the increase in phagocytosis was minimal to none. This could suggest that CD47 has additional roles in suppressing phagocytosis distinct from interactions with SIRPα. Alternatively, pharmacologic blockade may simply not prevent 100% of SIRPα binding. A third possibility is that homeostatic (and currently undefined) effects from knocking out CD47 somehow promote phagocytic proneness.

Previous studies have reported the induction of cytokine secretion, including murine monocyte chemotactic protein-3 (MCP-3),[3] in response to anti-CD47 therapy in vitro and in vivo. We identified induction of human IL-18 by TCL cells after anti-CD47 mAb treatment in separate in vivo models. IL-18 is a proinflammatory cytokine that can induce MCP-1/CCL2 production in macrophages through the phosphatidylinositol 3-kinase/AKT and MEK/extracellular signal-regulated kinase 1/2 pathways, and thereby stimulate recruitment.[24] Hence, it is conceivable that in the presence of CD47 antagonists, tumor cells secrete IL-18 that enhances production of cytokines such as MCP-1 to promote chemotactic migration and activation of macrophages. Several lines of evidence also suggest that IL-18 plays an important role in NK-cell differentiation and anti-tumor function.[29,30]

Although anti-CD47 treatments seem to induce dramatic antitumor responses in murine TCL models, there are some TCL lines such as the PTCL-NOS line SMZ1 that (as with $CD3^+$ T cells from healthy donors) exhibited intrinsic resistance to phagocytosis induction by anti-CD47 mAbs. Evaluation of other antiphagocytic regulators, such as surface expression of MHC class I or factors affecting pyroglutamation of CD47 cells, did not reveal obvious contributors to this resistance. Thus, further studies are needed to define mechanisms of resistance to phagocytosis and biomarkers that can be applied in patients with TCL and other diseases.

A limitation of PDX models in NSG mice, which lack B, T, and NK cells, is that these mice do not capture many aspects of in-human response to CD47 antagonists. The binding affinity of the NOD SIRPα to human CD47 is also 10-fold greater than the human SIRPα-human CD47 interaction. This could have confounding effects on the extent of phagocytosis induced by CD47-blocking agents across the diverse murine models.[31,32] To begin addressing activity in an immunocompetent background, we demonstrated that CD47 blockade is also effective in WT mice engrafted with ITK-SYK-expressing TCL cells. However, this approach is also confounded by the differences we observed between murine and human macrophages. Thus, future studies performed in humanized mice could help address the contributions of NK cell and adaptive immune responses to the efficacy of CD47 mAbs in vivo. In particular, the ability of CD47 blockade to affect dendritic cell phagocytosis and priming of T cells remains poorly understood.

Our data add to the emerging literature that blockade of CD47-SIRPα interaction is not adequate to optimally stimulate phagocytosis of tumor cells.[33] These data are also consistent with the clinical trial experience showing improved efficacy of anti-CD47 therapeutics when used in combination with other monoclonal antibodies. The clinical agent we used in these studies, SRF231, is under investigation in a phase 1 clinical trial for advanced malignancies (NCT03512340). Our data suggest that combinations with IgG1 mAbs are needed to maximize efficacy through ADCC and ADCP.

Acknowledgments

The authors thank Jurgen Ruland (Technical University of Munich) for his generous gift of the ITK-SYK lymphoma cells and members of the Weinstock laboratory for thoughtful discussion and assistance.

This work was supported by funding from the Leukemia and Lymphoma Society Specialized Center of Research (#7011-16), Surface Oncology to D.M.W. and F.W.L., and National Institutes of Health (R01 HL125780) (F.W.L.). S.J. is supported by the T-cell Leukemia Lymphoma Foundation Young Investigator Grant.

Authorship

Contribution: S.J., F.W.L., and D.M.W. designed the research; S.J., A.V.S., A.M., G.N., A.A., F.P., and G.P. performed the research; S.J., E.A.M., K.S., A.L., J.C.A., F.W.L., and D.M.W. analyzed data; S.J. and D.M.W. wrote the paper.

Conflict-of-interest disclosure: D.M.W. and F.W.L. received research funding from Surface Oncology. The remaining authors declare no competing financial interests.

ORCID profiles: S.J., 0000-0003-1566-9308; E.A.M., 0000-0001-5880-9337; D.M.W., 0000-0002-8724-3907.

Correspondence: David Weinstock, Dana-Farber Cancer Institute, 450 Brookline Ave, Dana 510B, Boston, MA 02215; e-mail: dweinstock@partners.org.

Footnotes

Submitted 24 May 2019; accepted 30 July 2019. Prepublished online as *Blood* First Edition paper, 5 August 2019; DOI 10.1182/blood.2019001744.

Presented in abstract form at the 60th annual meeting of the American Society of Hematology, San Diego, CA, 2 December 2018.

The online version of this article contains a data supplement.

There is a *Blood* Commentary on this article in this issue.

All primary data from RNA-seq as previously reported is available at https://portal.gdc.cancer.gov/legacy-archive/search/f and have been deposited in the National Center for Biotechnology Information's Gene Expression Omnibus (GSE114085). Mutation and RNA-seq data for PDXs are also available at www.PRoXe.org. All other remaining data are available within the article and supplemental files, including detailed description of the tissue microarray (TMA), or freely available from the authors upon request.

The publication costs of this article were defrayed in part by page charge payment. Therefore, and solely to indicate this fact, this article is hereby marked "advertisement" in accordance with 18 USC section 1734.

REFERENCES

1. Majeti R, Chao MP, Alizadeh AA, et al. CD47 is an adverse prognostic factor and therapeutic antibody target on human acute myeloid leukemia stem cells. *Cell*. 2009;138(2):286-299.
2. Chao MP, Alizadeh AA, Tang C, et al. Anti-CD47 antibody synergizes with rituximab to promote phagocytosis and eradicate non-Hodgkin lymphoma. *Cell*. 2010;142(5):699-713.
3. Weiskopf K, Jahchan NS, Schnorr PJ, et al. CD47-blocking immunotherapies stimulate macrophage-mediated destruction of small-cell lung cancer. *J Clin Invest*. 2016;126(7):2610-2620.
4. Gholamin S, Mitra SS, Feroze AH, et al. Disrupting the CD47-SIRPα anti-phagocytic axis by a humanized anti-CD47 antibody is an efficacious treatment for malignant pediatric brain tumors. *Sci Transl Med*. 2017;9(381):2968.
5. Tseng D, Volkmer JP, Willingham SB, et al. Anti-CD47 antibody-mediated phagocytosis of cancer by macrophages primes an effective antitumor T-cell response. *Proc Natl Acad Sci USA*. 2013;110(27):11103-11108.
6. McCracken MN, Cha AC, Weissman IL. Molecular pathways: activating T cells after cancer cell phagocytosis from blockade of CD47 "don't eat me" signals. *Clin Cancer Res*. 2015;21(16):3597-3601.
7. Liu X, Pu Y, Cron K, et al. CD47 blockade triggers T cell-mediated destruction of immunogenic tumors. *Nat Med*. 2015;21(10):1209-1215.
8. Lin GHY, Charbonneau M, Chai V, et al. Intratumoral delivery of TTI-621 (SIRPaFc), a CD47-blocking immunotherapeutic, inhibits tumor growth and prolongs animal survival in a subcutaneous B-cell lymphoma model [abstract]. *Cancer Res*. 2017;77(13 suppl). Abstract 2646.
9. Linderoth E, Helke S, Lee V, et al. The anti-myeloma activity of TTI-621 (SIRPαFc), a CD47-blocking immunotherapeutic, is enhanced when combined with a proteasome inhibitor [abstract]. *Cancer Res*. 2017;77(13 suppl). Abstract 2653.
10. Ring NG, Herndler-Brandstetter D, Weiskopf K, et al. Anti-SIRPα antibody immunotherapy enhances neutrophil and macrophage anti-tumor activity. *Proc Natl Acad Sci USA*. 2017;114(49):E10578-E10585.
11. Agoram B, Wang B, Sikic BI, et al. Pharmacokinetics of Hu5F9-G4, a first-in-class anti-CD47 antibody, in patients with solid tumors and lymphomas [abstract]. *J Clin Oncol*. 2016;36(15_suppl):2525. Abstract 2525.
12. Advani R, Flinn I, Popplewell L, et al. CD47 blockade by Hu5F9-G4 and rituximab in non-Hodgkin's lymphoma. *N Engl J Med*. 2018;379(18):1711-1721.
13. Petrova PS, Viller NN, Wong M, et al. TTI-621 (SIRPαFc): A CD47-blocking innate immune checkpoint Inhibitor with broad antitumor activity and minimal erythrocyte binding. *Clin Cancer Res*. 2017;23(4):1068-1079.
14. Querfeld C, Thompson JA, Taylor M, et al. A single direct intratumoral injection of TTI-621 (SIRPαFc) induces antitumor activity in patients with relapsed/refractory mycosis fungoides and Sézary syndrome: preliminary findings employing an immune checkpoint inhibitor blocking the CD47 "do not eat" signal [abstract]. *Blood*. 2017;130:4076. Abstract 4076.
15. Kauder SE, Kuo TC, Harrabi O, et al. ALX148 blocks CD47 and enhances innate and adaptive antitumor immunity with a favorable safety profile. *PLoS One*. 2018;13(8):e0201832.
16. Lakhani NJ, LoRusso P, Hafez N, et al. A phase I study of ALX148, a CD47 blocker, alone and in combination with established anticancer antibodies in patients with advanced malignancy and non-Hodgkin lymphoma [abstract]. *J Clin Oncol*. 2018;36(15_suppl):3068. Abstract 3068.
17. Sallman DA, Donnellan WB, Asch AS, et al. The first-in-class anti-CD47 antibody Hu5F9-G4 is active and well tolerated alone or with azacytidine in AML and MDS patients: initial phase 1b results [abstract]. *J Clin Oncol*. 2019:37:7009. Abstract 7009.
18. Barkal AA, Weiskopf K, Kao KS, et al. Engagement of MHC class I by the inhibitory receptor LILRB1 suppresses macrophages and is a target of cancer immunotherapy. *Nat Immunol*. 2018;19(1):76-84.
19. Chen J, Zhong MC, Guo H, et al. SLAMF7 is critical for phagocytosis of haematopoietic tumour cells via Mac-1 integrin. *Nature*. 2017;544(7651):493-497.
20. Logtenberg MEW, Jansen JHM, Raaben M, et al. Glutaminyl cyclase is an enzymatic modifier of the CD47- SIRPα axis and a target for cancer immunotherapy. *Nat Med*. 2019;25(4):612-619.
21. Ng SY, Yoshida N, Christie AL, et al. Targetable vulnerabilities in T- and NK-cell lymphomas identified through preclinical models. *Nat Commun*. 2018;9(1):2024.
22. Challa-Malladi M, Lieu YK, Califano O, et al. Combined genetic inactivation of β2-Microglobulin and CD58 reveals frequent escape from immune recognition in diffuse large B cell lymphoma. *Cancer Cell*. 2011;20(6):728-740.
23. Pechloff K, Holch J, Ferch U, et al. The fusion kinase ITK-SYK mimics a T cell receptor signal and drives oncogenesis in conditional mouse models of peripheral T cell lymphoma. *J Exp Med*. 2010;207(5):1031-1044.
24. Yoo JK, Kwon H, Khil LY, Zhang L, Jun HS, Yoon JW. IL-18 induces monocyte chemotactic protein-1 production in macrophages through the phosphatidylinositol 3-kinase/Akt and MEK/ERK1/2 pathways. *J Immunol*. 2005;175(12):8280-8286.
25. Takai T, Li M, Sylvestre D, Clynes R, Ravetch JV. FcR γ chain deletion results in pleiotrophic effector cell defects. *Cell*. 1994;76(3):519-529.
26. Coxon A, Rieu P, Barkalow FJ, et al. A novel role for the beta 2 integrin CD11b/CD18 in neutrophil apoptosis: a homeostatic mechanism in inflammation. *Immunity*. 1996;5(6):653-666.
27. He Y, Bouwstra R, Wiersma VR, et al. Cancer cell-expressed SLAMF7 is not required for CD47-mediated phagocytosis. *Nat Commun*. 2019;10(1):533.
28. Kim YH, Bagot M, Pinter-Brown L, et al; MAVORIC Investigators. Mogamulizumab versus vorinostat in previously treated cutaneous T-cell lymphoma (MAVORIC): an international, open-label, randomised, controlled phase 3 trial. *Lancet Oncol*. 2018;19(9):1192-1204.
29. Molgora M, Bonavita E, Ponzetta A, et al. IL-1R8 is a checkpoint in NK cells regulating anti-tumour and anti-viral activity. *Nature*. 2017;551(7678):110-114.
30. Takeda K, Tsutsui H, Yoshimoto T, et al. Defective NK cell activity and Th1 response in IL-18-deficient mice. *Immunity*. 1998;8(3):383-390.
31. Subramanian S, Boder ET, Discher DE. Phylogenetic divergence of CD47 interactions with human signal regulatory protein α reveals locus of species specificity. Implications for the binding site. *J Biol Chem*. 2007;282(3):1805-1818.
32. Kwong LS, Brown MH, Barclay AN, Hatherley D. Signal-regulatory protein α from the NOD mouse binds human CD47 with an exceptionally high affinity–implications for engraftment of human cells. *Immunology*. 2014;143(1):61-67.
33. Veillette A, Chen J. SIRPα-CD47 immune checkpoint blockade in anticancer therapy. *Trends Immunol*. 2018;39(3):173-184.